

ARTICLE

Intermolecular Hydroamination Catalysed by Alkali Metal Magnesiates

Received 00th January 20xx,
Accepted 00th January 20xx

Laia Davin, Alberto Hernán-Gómez, Calum McLaughlin, Alan R. Kennedy, Ross McLellan and Eva Hevia*

DOI: 10.1039/x0xx00000x

Main group bimetallic complexes, while being increasingly used in stoichiometric deprotonation and metal-halogen exchange reactions, have largely been overlooked in catalytic applications. This paper explores the ability of alkali metal magnesiates to catalyse the intermolecular hydroamination of alkynes and alkenes using diphenylacetylene and styrene as model substrates. By systematically studying the role of the alkali-metal and the formulation of the heterobimetallic precatalyst, this study establishes higher order potassium magnesiate ($[(\text{PMDETA})_2\text{K}_2\text{Mg}(\text{CH}_2\text{SiMe}_3)_4]$ (**7**) as a highly effective system capable of catalysed the hydroamination of styrene and diphenylacetylene with several amines while operating at room temperature. This high reactivity contrast with the complete lack of catalytic ability of neutral $\text{Mg}(\text{CH}_2\text{SiMe}_3)_2$, even when harsher reaction conditions are employed (24h, 80°C). Through stoichiometric reactions, and structural and spectroscopic (DOSY NMR) investigations we shed some light on the potential reaction pathway as well as the constitution of key intermediates. These studies suggest that the enhanced catalytic activity of **7** can be rationalised in terms of the superior nucleophilic power of the formally dianionic magnesiate $\{\text{Mg}(\text{NR}_2)_4\}^{2-}$ generated in situ during the hydroamination process, along with the ability of potassium to engage in π -interactions with the unsaturated organic substrate, enhancing its susceptibility towards a nucleophilic attack by the amide anion.

Introduction

Hydroamination reactions are described as the addition of an N-H fragment across an unsaturated C-C bond. They constitute one of the most powerful atom-efficient and waste-minimized methodologies to access amines in organic synthesis.¹ Such nitrogen-containing species have a great importance as lead structures among numerous pharmaceuticals, biological systems, natural products and industrially basic and fine chemicals.² However, the high kinetic hurdle of these processes imposes in most cases the use of metal catalysts.³ Over the last two decades, transition-metal systems such as rhodium, ruthenium, titanium or palladium have seen significant progress due to their good tolerance of polar functional groups.⁴ Pioneering work by the groups of Hill and Harder have revealed that alkaline earth metal (particularly calcium and strontium) complexes, cheaper and more sustainable synthetic alternatives, can also act as catalysts in intramolecular as well as the more challenging intermolecular hydroamination reactions.⁵ Moreover, these reactions frequently occur under relatively mild conditions. Work by Hill, Carpentier and Sarazin

have also disclosed that the catalyst activity increases with increasing ionic radius of the metal, revealing that magnesium displays poor reactivity.^{5b,6} A similar effect was observed in organolanthanide hydroamination catalysis, reported by Marks.^{1b,7} Reports of alkali metal based catalysts are much more scarce, although *sec*-BuLi or Na metal has been known since the 1950's.^{1a,2a,3d,8} Notably alkali-metal catalysed hydroamination reactions impose harsh reaction conditions (high temperatures long reaction times).

Mechanistically, it is suggested that alkaline earth metal catalysed processes proceed through a metal amide intermediate, followed by substrate insertion into the M-N bond, since these main group metals cannot operate via oxidative addition / reductive elimination steps observed with transition metal catalysts. In these examples it is suggested that activation of the unsaturated organic fragment takes place by forming electrostatic interactions with the group II metal, which leads to the polarization of the π -electron density, facilitating the nucleophilic attack by the amide group.³

Bimetallic catalysts are emerging as alternatives to the more conventional single-metal catalytic transformations, providing enhanced selectivity and reactivity in a variety of processes.⁹ Key to their success is the proximity of the two metals, affording scenarios where they operate synergically. The vast majority of bimetallic catalysts developed involved transition-metals whereas the number of examples using main-group metal systems is very limited.¹⁰ Within alkali-metal magnesiates, unique cooperativity arises because one metal (here an alkali metal) can act as a Lewis acid allowing the activation of the

Dr L. Davin, Dr A. Hernán-Gómez, C. McLaughlin Dr A. R. Kennedy, Dr R. McLellan, Prof. E. Hevia

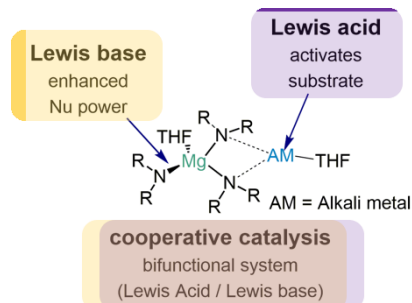
WestCHEM, Department of Pure and Applied Chemistry
University of Strathclyde
Glasgow, G1 1XL (UK)

E-mail: eva.hevia@strath.ac.uk

† This is a peer reviewed accepted author manuscript of the following research article: Davin, L., Hernán-Gómez, A., McLaughlin, C., Kennedy, A. R., McLellan, R., & Hevia, E. (2019). Alkali metal and stoichiometric effects in intermolecular hydroamination catalysed by lithium, sodium and potassium magnesiates. *Dalton Transactions*, 48(23), 8122-8130. <https://doi.org/10.1039/C9DT00923J>

unsaturated organic substrate facilitating the intramolecular nucleophilic attack by the highly nucleophilic Lewis basic tris(magnesiate) anion (Figure 1).

Figure 1 Generic depiction of a cooperative bimetallic alkali metal magnesiate catalyst.



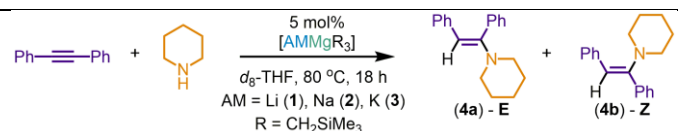
Recently we have shown magnesium activated within a sodium magnesiate platform can outperform Ca and Ba systems for the hydroamination of isocyanates, giving higher yields and superior substrate scope under milder reaction conditions.¹¹ Using homoleptic tris(alkyl) sodium magnesiate [NaMg(CH₂SiMe₃)₃] as a precatalyst, these studies suggest that the reaction takes place with the initial formation of a highly reactive tris(amido) species, which in turn undergoes nucleophilic addition to the unsaturated electrophile RNC=O. Prior coordination of RNC=O to the Lewis acidic sodium centre, activates the nucleophilic substitution step. We have also reported the applications of this mixed Na/Mg system as an efficient precatalyst for the guanylation and hydrophosphination of amines, proceeding by a similar reaction pathway.¹² Related to these findings, Westerhausen has demonstrated that potassium calciates [K₂Ca(NPh₂)₄] and [K₂Ca{(N(H)Dipp)}₄] can catalyse the hydroamination reactions of diphenylbutadiyne with a variety of anilines.¹³ Exemplifying the cooperative effect of the ate compound as a catalyst, no reaction product is observed when adding diphenylamine to 1,4-diphenylbutadiyne in presence of Ca(NPh₂)₂ or KNPh₂. However, when the bimetallic calciate compound K₂Ca(NPh₂)₄ is used as a catalyst the hydroamination products are formed in a >90% NMR yield (Z isomer 40.4%, isolated yield).

Expanding wider the catalytic applications of s-block bimetallics, herein we systematically investigate the ability of a range of alkali-metal magnesiates to catalyse intermolecular hydroamination of alkynes and alkenes using diphenylacetylene and styrene as model substrates. Combining catalytic studies with stoichiometric, structural and spectroscopic investigations, the roles of the alkali-metal and the constitution of the magnesiate anion have been assessed, providing new mechanistic insights into s-block cooperative catalysis.

Results and discussion

We first assessed the intermolecular hydroamination of diphenylacetylene with piperidine, catalysed by trisalkyl (or lower order) alkali-metal magnesiates, that is, complexes of the formula AMMg(CH₂SiMe₃)₃ (AM = alkali metal = Li, Na, K),

prepared by simple co-complexation of AMCH₂SiMe with Mg(CH₂SiMe₃)₂.¹⁴ Reaction using LiMg(CH₂SiMe₃)₃ (**1**) with 5 mol % loading in *d*₈-THF afforded 49% yield of hydroamination product after heating at 80 °C for 18 hours. Furthermore, the reaction proceeded with reasonable stereoselectivity favouring the E- over the Z-isomer by 86:14 (Table 1 entry 1). Repeating the reaction with NaMg(CH₂SiMe₃)₃ (**2**) and KMg(CH₂SiMe₃)₃ (**3**) under the same conditions (entries 2-3) affords a markedly increased yield when catalysed by **2** (98%) and a slightly increased yield when **3** is used as the catalyst (59%). Furthermore, when **2** is used the selectivity decreases E:Z (70:30). This clear alkali metal effect is interesting since reactivity does not seem to follow a trend in line with the radius of the alkali metal, suggesting that some more subtle effects are in operation. Previously it has been noted through experimental and theoretical calculations on group 2 complexes, that the metal polarisability, charge density as well as size can greatly influence the outcome in main-group catalysis.¹⁵ Thus we postulate that a similar scenario is occurring in the present work.^{5b} Despite the promise of our best performing catalyst **2** in hydroamination, it is outperformed by the strontium catalyst [Sr{CH(SiMe₃)₂]₂(THF)₂ reported by Hill.^{5e} In this example quantitative yields are obtained after only two hours at 60°C, with high E:Z selectivity (91:9). Thus, we decided to investigate the role of catalyst loading and solvent, in an effort to optimise the process. Firstly, repeating the intermolecular hydroamination reaction between diphenylacetylene and piperidine with different loadings of **2** reveals that the loading can be reduced to 2 mol% without any drop-off in reactivity. Next, we repeated the reaction in CDCl₃ and C₆D₆ (entries 6-7). In the former case no reactivity is observed, whereas in the latter only 42% of hydroamination product is obtained with an E:Z selectivity of (90:10).



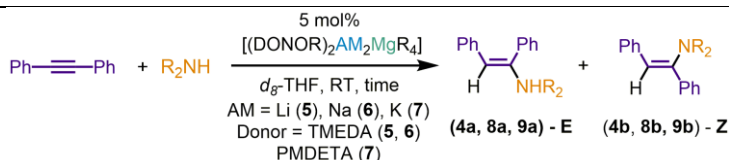
Entry	AM	Solvent	Yield (%) ^[a]	E:Z ^[b]
1	Li	<i>d</i> ₈ -THF	48	86:14
2	Na	<i>d</i> ₈ -THF	98	70:30
3	K	<i>d</i> ₈ -THF	59	84:16
4 ^[c,e]	Na	<i>d</i> ₈ -THF	100	63:37
5 ^[d,e]	Na	<i>d</i> ₈ -THF	97	66:34
6 ^[e]	Na	CDCl ₃	0	-
7 ^[e]	Na	C ₆ D ₆	42	90:10

Table 1 Intermolecular hydroamination of diphenylacetylene with piperidine, catalysed by lower order alkali metal magnesiates. [a] Yields determined by ¹H NMR using ferrocene as an internal standard. [b] Determined by ¹H NMR spectroscopy. [c] 10 mol% loading. [d] 2 mol% loading. [e] 15 hours.

Encouraged by the initial results using homoleptic triorganomagnesiates (**1-3**) we next studied the ability of the higher order derivatives [(TMEDA)₂Li₂Mg(CH₂SiMe₃)₄] (**5**)^{14a} [(TMEDA)₂Na₂Mg(CH₂SiMe₃)₄] (**6**)^{16a} and [(PMDETA)₂K₂Mg(CH₂SiMe₃)₄] (**7**), all of which containing a formally dianionic magnesiate fragment.^{16b} Previous studies of

these tetraorgano complexes revealed that they demonstrate significantly enhanced reactivity in deprotonative metalation¹⁷ and Mg-halogen¹⁸ exchange than their lower order counterparts. Once more we began by studying the intermolecular hydroamination reaction between diphenylacetylene with piperidine, catalysed by **5-7** (5 mol%). When **5** is used as a catalyst at room temperature in d_8 -THF, no reaction occurs over a 3-hour period (Table 2 entry 1). In contrast, when catalysed by **6**, only 28% of hydroamination product is obtained in an E:Z ratio of 29:71 (entry 2). Contrastingly a remarkable increase in reactivity and selectivity is observed when employing mixed K/Mg precatalyst **7** affording hydroamination products **4a-b** in almost quantitative yields with a greater E/Z selectivity (93:7, entry 3). These results uncover an even more dramatic alkali-metal effect than when using triorganomagnesiates **1-3** (*vide supra*). Furthermore, the enhanced nucleophilic character of **5-7** enables hydroamination of diphenylacetylene to take place at room temperature. These reaction conditions are remarkable as even reactive heavier alkaline-earth metal systems require higher temperatures for the hydroamination process to occur.^{5e} Reflecting the importance of the K/Mg partnership in **7**, when monometallic neutral magnesium $Mg(CH_2SiMe_3)_2$ is used as a precatalyst, no hydroamination occurs, even after heating at 80 °C for 24 hours (entry 4, table 2). In an attempt to glean some information into the role of potassium in this transformation we reacted diphenylacetylene with piperidine using **7**, in the presence of an additional 10 mol% of 18-crown-6 (entry 5). Since 18-crown-6 has a high affinity for potassium ions, we rationalised that in the presence of the macrocycle we would saturate the coordination of the alkali metal, thereby preventing access of the substrate and slowing down the reaction. Monitoring the reaction via ¹H NMR spectroscopy revealed that even after heating at 80 °C for 24 hours no reaction occurs. This result therefore implies that the level of potassium coordination effects its key role as a Lewis acid, enabling activation of the unsaturated molecule and facilitating the nucleophilic addition by bringing it into close proximity to the anionic amido-magnesiates intermediate. In contrast, guanylation reactions catalysed by **2**, only show a slight decrease in reactivity after the addition of 15-crown-5 suggesting a secondary role of the alkali-metal in this process.¹³ This is consistent with the formation of solvent separated ion pair species in solutions, whereas in here reactions seem to take place via the formation of contacted ion pair species which facilitate metal-metal communication between potassium and magnesium.

Satisfied with the excellent catalytic ability of **7**, we next sought to examine the scope of amines suitable for this reaction (Table 2 entries 6-9). Hydroamination of diphenylacetylene with six or five membered cyclic amines piperidine and pyrrolidine is fast at room temperature when catalysed by **7**, taking 3 or 2 hours respectively for full conversion. Installing an oxygen atom into the six-membered ring of piperidine has a profound effect on the efficiency of catalysis. Thus entry 7 shows that morpholine requires 24 hours at room temperature



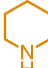
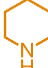
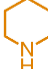
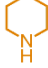
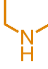

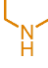
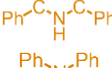

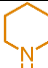

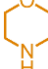
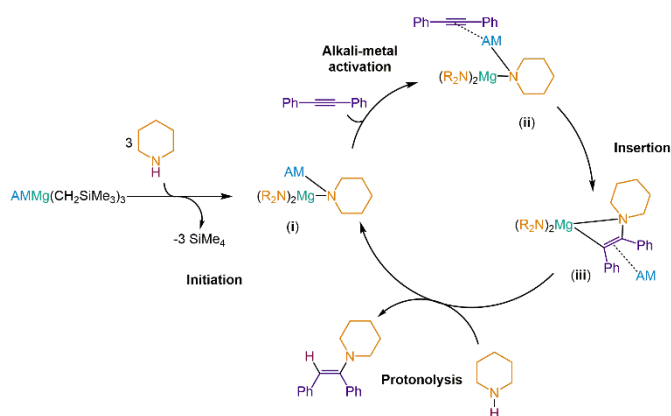
Entry	Amine	AM	Time (h)	Yield (%) ^[a]	E:Z ^[b]
1		Li	3	0	-
2		Na	3	28	29:71
3		K	3	≥99	93:7
4 ^[c]		MgR ₂	24	0	-
5 ^[c]		K + 18-Cr-6 (10 mol%)	24	0	-
6		K	2	≥99	94:6
7		K	24	80	92:8
8 ^[c]		K	24	0	-
9 ^[c]		K	24	0	-
$\text{Styrene} + \text{R}_2\text{NH} \xrightarrow[\text{d}_8\text{-THF, RT, time}]{\text{5 mol\% } [(\text{PMDETA})_2\text{K}_2\text{MgR}_4] \text{ (7)}}$					
10		7	0.25	≥99	
11		7	0.25	≥99	
12		7	0.25	≥99	

Table 2 Intermolecular hydroamination of diphenylacetylene and styrene catalysed by higher order alkali metal magnesiates. [a] Yields determined by ¹H NMR using ferrocene as an internal standard. [b] Determined by ¹H NMR spectroscopy. [c] 80 °C.

to afford the hydroamination product in 80% (E:Z 92:8). Notably the same reactions are reported using nickel or gold catalysts, however long timescales and high temperatures are necessary.¹⁹ Hydroamination reactions using less nucleophilic amines, dibenzylamine and diphenylamine do not occur. ¹H NMR monitoring of these reactions is consistent with the *in situ* formation of a {K₂Mg(amide)₄} intermediate, which appears not to be active enough to facilitate the amide addition to the C-C triple bond. **7** is also a capable catalyst in the

hydroamination of styrene. In these examples (entries 10-12), piperidine, pyrrolidine and morpholine all give complete hydroamination within 15 minutes at room temperature, affording selectively the anti-Markovnikov product. That these reactions proceed instantly, and much more rapidly than the hydroamination of diphenylacetylene, indicate that steric congestion may play a key role in whether the reaction is feasible. In contrast to our findings, other reports have shown that high temperatures and long timescales are required for these reactions. For example, $\text{LiN}(\text{SiMe}_3)_2$ (5 mol%) in the presence of TMEDA (5 mol%) in C_6D_6 at 120 - 150 °C, affords the hydroamination products after 1 – 3 hours in 61-82 % yields.^{8a} Group 2 catalysts such as $[\text{Sr}\{\text{CH}(\text{SiMe}_3)_2\}_2(\text{THF})_2]$ achieve the piperidine hydroamination product in 70% yield after 10 minutes at room temperature, using 5 mol% of the strontium precatalyst.^{5e} Satisfied that both the lower order (specifically **2**) and higher order (specifically **7**) alkali-metal magnesiate are efficient catalysts in these intermolecular hydroamination reactions, we next set out to discover some structural and spectroscopic insight into the nature of potentially active catalytic intermediates. Hill proposed a mechanism for the alkaline earth catalysed intermolecular hydroamination,^{5e} and suggested that they operate in a similar manner to early transition metal complexes.²⁰ Using this proposal as a starting point for our studies using heterobimetallic complexes we propose that the reaction proceeds as follows (Scheme 1): 1/ the alkali-metal magnesiate deprotonates the amine, thereby initiating the reaction by generating a sufficiently nucleophilic magnesium amide (i) and losing SiMe_4 ; 2/ the presence of the alkali-metal next activates the π -system of the substrate molecule drawing it into the proximity of the nucleophile and priming it for insertion (ii); 3/ substrate insertion into the magnesium-nitrogen bond giving iii; 4/ protonolysis to regenerate the active alkali-metal amido magnesiate. Since our experimental results demonstrate a dramatic alkali metal effect, the catalyst selection is crucial in activating the unsaturated substrate for onward reaction.



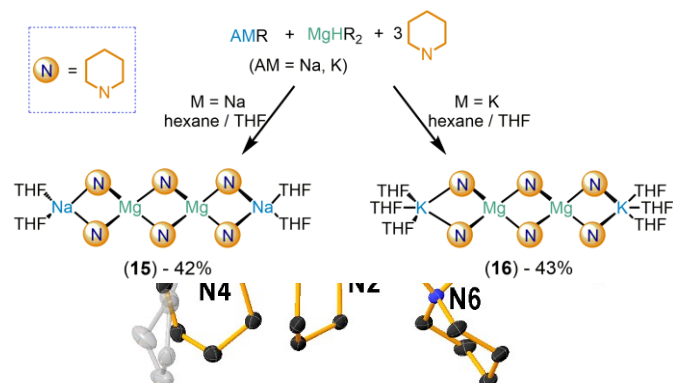
Scheme 1 Proposed catalytic cycle for intermolecular hydroamination reactions via metal amide species catalysed by alkali-metal magnesiate catalysts. Lower order alkali-metal magnesiate is depicted here for illustrative purposes.

With these steps in mind we conducted a series of stoichiometric reactions between **2**, **3**, **6** and **7** with piperidine.

2 and **3** were prepared *in situ* by mixing the monometallic reagents $\text{MCH}_2\text{SiMe}_3$ ($\text{M} = \text{Na}, \text{K}$) and $\text{Mg}(\text{CH}_2\text{SiMe}_3)_2$ in a 1:1 ratio in hexane (Scheme 2). Subsequently, of 3 equivalents of piperidine were added, followed by small amount of THF to solubilise the white precipitate. Single crystals of $[(\text{THF})_2(\text{NaMg}(\text{NC}_5\text{H}_{10})_3)]_2$ (**15**) and $[(\text{THF})_3(\text{KMg}(\text{NC}_5\text{H}_{10})_3)]_2$ (**16**) were grown in 42% and 43% yield respectively.

Scheme 2 Synthesis of lower order sodium and potassium amidomagnesiate **15** and **16**.

The single-crystal X-ray structures of **15** and **16** are very similar although the poor quality of the latter precludes discussion of geometric parameters. Compound **15** displays a dimeric



contacted ion-pair structure (Figure 2) where the metals adopt a pseudolinear $[\text{NaMgMgNa}]$ arrangement ($\text{Na}_2 \cdots \text{Mg}_1 \cdots \text{Mg}_2$, 158.48(3)° and $\text{Mg}_1 \cdots \text{Mg}_2 \cdots \text{Na}_1$, 161.77(3)°).

Figure 2 Molecular structure of **15** with 30% probability displacement ellipsoids. All hydrogen atoms have been omitted for clarity.

The distorted tetrahedral Mg centres bind to four μ -piperidide groups (average Mg-N 2.10(3) Å), anchoring the structure, whereas distorted tetrahedral Na is affixed to the $\{\text{MgN}(\text{C}_5\text{H}_{10})_4\}$ component forming elongated ancillary bonds (mean Na-N, 2.46(1) Å). Two solvating molecules of THF complete the coordination sphere of each sodium atom. This concept of anchoring/ancillary bonding has been previously described for bimetallic compounds.²¹ The central $[\text{MgNMgN}]$ four-membered planar ring is orthogonal to two adjacent $[\text{NaNMgN}]$, and this structural motif of three fused four-membered rings, comprising a MMgMgM arrangement has been previously reported in the pioneering work of Weiss.²² Nevertheless the isolation of **15** and **16** provides strong evidence that amine deprotonation is the first step in the catalytic profile, and generates catalytically active species.

Probing these complexes further we decided to investigate their solution state properties **15** and **16** in d_8 -THF, via Diffusion Ordered Spectroscopy (DOSY), using the method recently reported by Stalke.²³ Using this method we are able to obtain a reliable molecular weight estimation of the species in solution, based upon their diffusion coefficients against a TMS as an internal standard (Figure 3). **15** has an estimated molecular weight of 694 g mol⁻¹ which is suggestive of a dimeric structure that resembles that observed in the solid state albeit with fewer

solvating THF molecules. The expected mass for **15** with one and two solvating THF molecules is 672 g mol^{-1} (-3% error) and 743 g mol^{-1} (7% error), indicating that on the DOSY timescale there is likely between 1 and two solvating THF molecules. The DOSY spectrum of **16** reveals very similar characteristics. The experiment gives a value of 734 g mol^{-1}

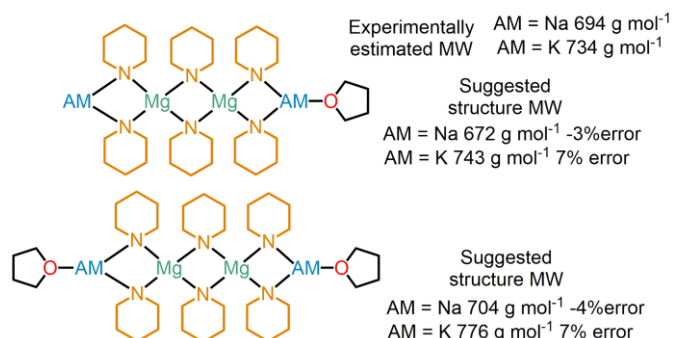
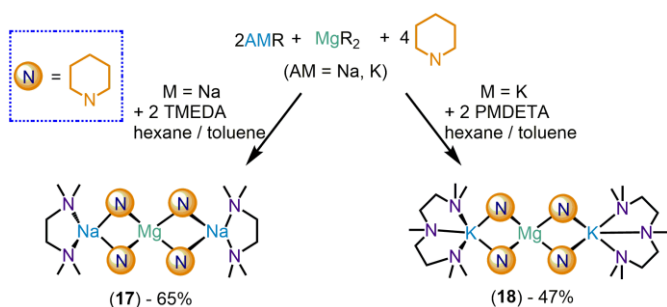


Figure 3 Suggested aggregation states of **15** and **16** in d_8 -THF solution, obtained from DOSY NMR studies.

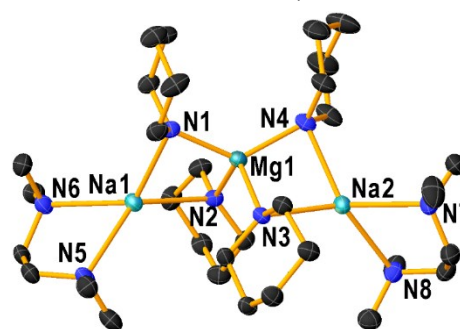
Following a similar procedure to the synthesis of **15** and **16**, except that $\text{MCH}_2\text{SiMe}_3$ ($M = \text{Na}, \text{K}$) and $\text{Mg}(\text{CH}_2\text{SiMe}_3)_2$ were mixed in a 2:1 ratio and 4 equivalents of piperidine were added in hexane/toluene, the higher order alkali-metal magnesiates $[(\text{TMEDA})_2\{\text{Na}_2\text{Mg}(\text{NC}_5\text{H}_{10})_4\}]$ **17** and $[(\text{PMDETA})_2\{\text{K}_2\text{Mg}(\text{NC}_5\text{H}_{10})_4\}]$ **18** were prepared as colourless crystals in 65% and 47% yields respectively (Scheme 3). **17** and **18** display the same core architecture, however, poor data quality prevents an accurate discussion of geometric parameters of **18**. In **17** a central distorted tetrahedral magnesium is connected to two peripheral alkali metal cations by 4 μ -piperidide ligands (Figure 4). The Na and K ions in **17** and **18** are further solvated by either TMEDA or PMDETA respectively. A search in the CCDC database revealed that other bimetallic amides have a similar core architecture. These include a lithium manganate²⁴ and only two higher order lithium amido-magnesiates.²⁵



Scheme 3 Synthesis of higher order sodium and potassium amidomagnesiates **17** and **18**.

Single crystal X-ray diffraction studies reveal that **17** and **18** Finally, in an effort to probe the insertion of the alkyne into the Mg-N bonds of **15-18** we conducted a series of stoichiometric experiments. Unfortunately, we were unable to effectively characterise such a species. Instead the only product we were able to observe was the final hydroamination product in each case, highlighting the instability/high reactivity of such an intermediate, and its propensity to react further in a product forming step.

Figure 4 Molecular structure of **17** with 30% probability displacement ellipsoids. All hydrogen atoms have been omitted for clarity



Experimental

General experimental:

All reactions and manipulations were conducted under a protective argon atmosphere using either standard Schlenk techniques or an MBraun glove box fitted with a gas purification and recirculation unit. NMR experiments were conducted in J. Young's NMR tubes oven dried and flushed with Argon prior to use. Hexane, toluene and THF were dried by heating to reflux temperature over sodium benzophenone ketyl and then distilled under nitrogen prior to use. All other reagents were purchased commercially from Sigma-Aldrich and dried via distillation from the appropriate drying agent prior to use.

NMR Spectroscopy: NMR spectra were recorded on a Bruker AV3 or AV 400 MHz spectrometer operating at 400.13 MHz for ^1H and 100.62 MHz for ^{13}C . All ^{13}C spectra were proton decoupled. ^1H and ^{13}C NMR spectra were referenced against the appropriate solvent signal.

X-ray Crystallography: Crystallographic data were collected on Oxford Diffraction instruments with Mo $K\alpha$ radiation ($\lambda = 0.71073 \text{ \AA}$) or Cu $K\alpha$ radiation ($\lambda = 1.54184 \text{ \AA}$). Structures were solved using SHELXS-97²⁶ while refinement was carried out on F2 against all independent reflections by the full matrix least-squares method using the SHELXL-97. All non-hydrogen atoms were refined using anisotropic thermal parameters. Selected crystallographic details and refinement details are provided in table S1. CCDC XXXXX-XXXXX contains the supplementary crystallographic data for these structures. These data can be obtained free of charge from the Cambridge Crystallographic Data Centre via www.ccdc.cam.ac.uk/data_request/cif.

Synthetic procedures

General procedure for catalytic hydroamination reactions: In a glovebox, the NMR tube was filled with 0.6 mmol of amine, 0.5 mmol of alkene or alkyne, 10 mol% of ferrocene (0.0095 g, 0.05 mmol) as internal standard and 0.609 g of solvent. The initial ratio of starting materials was calculated by integration of the ^1H NMR spectrum relative to the ferrocene. The precatalyst (2, 5 or 10 mol%) was introduced and the reactions times were measured from this point in regular intervals until full conversion by ^1H NMR spectrum (some reactions were heated in a pre-heated oil bath). All the yields were calculated by

integration of the products relative to the ferrocene in the ^1H NMR spectrum.

Characterisation of 1-(1,2-diphenylvinyl)piperidine (4a): ^1H NMR (400.13 MHz, d_8 -THF, 298 K) δ 7.36-7.16 [m, 5H, H_{ar}], 6.95-6.70 [m, 5H, H_{ar}], 5.62 [s, 1H, C=CH], 2.90-2.82 [m, 4H, $\text{N}(\text{CH}_2\text{CH}_2)_2\text{CH}_2$], 1.64-1.49 [m, 6H, $\text{N}(\text{CH}_2\text{CH}_2)_2\text{CH}_2$]. ^{13}C NMR (400.13 MHz, d_8 -THF, 298 K) δ 153.0 [C=C-N], 140.4 [C_{q}], 139.3 [C_{q}], 131.2 [CH], 129.2 [CH], 129.1 [CH], 128.7 [CH], 128.3 [CH], 124.7 [CH], 107.0 [C=CH], 51.2 [$\text{N}(\text{CH}_2\text{CH}_2)_2\text{CH}_2$], 27.2 [$\text{N}(\text{CH}_2\text{CH}_2)_2\text{CH}_2$], 25.4 [$\text{N}(\text{CH}_2\text{CH}_2)_2\text{CH}_2$].

Characterisation of 1-(1,2-diphenylvinyl)pyrrolidine (8a): ^1H NMR (400.13 MHz, d_8 -THF, 298 K) δ 7.34-7.21 [m, 5H, H_{ar}], 6.89-6.59 [m, 5H, H_{ar}], 5.35 [s, 1H, C=CH], 3.07-2.95 [m, 4H, $\text{N}(\text{CH}_2\text{CH}_2)_2$], 1.88-1.76 [m, 4H, $\text{N}(\text{CH}_2\text{CH}_2)_2$]. ^{13}C NMR (400.13 MHz, d_8 -THF, 298 K) δ 148.7 [C=C-N], 140.4 [C_{q}], 139.2 [C_{q}], 130.3 [CH], 129.1 [CH], 128.1 [CH], 127.9 [CH], 123.2 [CH], 100.7 (C=CH), 49.1 [$\text{N}(\text{CH}_2\text{CH}_2)_2$], 25.6 [$\text{N}(\text{CH}_2\text{CH}_2)_2\text{CH}_2$].

Characterisation of 1-(1,2-diphenylvinyl)morpholine (9a): ^1H NMR (400.13 MHz, d_8 -THF, 298 K) δ 7.37-7.21 [m, 5H, H_{ar}], 6.99-6.71 [m, 5H, H_{ar}], 5.63 [s, 1H, C=CH], 3.71-3.59 [m, 4H, $\text{N}(\text{CH}_2\text{CH}_2)_2\text{O}$], 2.89-2.77 [m, 4H, $\text{N}(\text{CH}_2\text{CH}_2)_2\text{O}$]. ^{13}C NMR (400.13 MHz, d_8 -THF, 298 K) δ 151.9 [C=C-N], 139.7 [C_{q}], 138.2 [C_{q}], 132.3 [C_{q}], 131.2 [CH], 129.2 [CH], 128.8 [CH], 128.2 [CH], 124.7 [CH], 107.0 [C=CH], 50.5 [$\text{N}(\text{CH}_2\text{CH}_2)_2\text{O}$], 47.7 [$\text{N}(\text{CH}_2\text{CH}_2)_2\text{O}$].

Characterisation of 1-phenethylpiperidine (12): ^1H NMR (400.13 MHz, CDCl_3 , 298 K) δ 7.35-7.39 [m, 2H, H_{ar}], 7.28-7.31 [m, 3H, H_{ar}], 2.90-2.94 [m, 2H, $\text{PhCH}_2\text{CH}_2\text{N}$], 2.64-2.68 [m, 2H, $\text{PhCH}_2\text{CH}_2\text{N}$], 2.57 [bs, 4H, $\text{N}(\text{CH}_2\text{CH}_2)_2\text{CH}_2$], 1.74 [m, 4H, $\text{N}(\text{CH}_2\text{CH}_2)_2\text{CH}_2$], 1.53-1.60 [m, 2H, $\text{N}(\text{CH}_2\text{CH}_2)_2\text{CH}_2$]. ^{13}C NMR (400.13 MHz, CDCl_3 , 298 K) δ 140.4 [C_{q}], 128.4 [CH], 128 [CH], 125.8 [CH], 61.1 [$\text{PhCH}_2\text{CH}_2\text{N}$], 54.5 [$\text{N}(\text{CH}_2\text{CH}_2)_2\text{CH}_2$], 33.4 [$\text{PhCH}_2\text{CH}_2\text{N}$], 25.8 [$\text{N}(\text{CH}_2\text{CH}_2)_2\text{CH}_2$], 24.19 [$\text{N}(\text{CH}_2\text{CH}_2)_2\text{CH}_2$].

Characterisation of 1-phenethylpyrrolidine (13): ^1H NMR (400.13 MHz, CDCl_3 , 298 K) δ 7.34-7.40 [m, 2H, H_{ar}], 7.27-7.33 [m, 3H, H_{ar}], 2.94 [m, 2H, $\text{PhCH}_2\text{CH}_2\text{N}$], 2.80 [m, 2H, $\text{PhCH}_2\text{CH}_2\text{N}$], 2.63-2.71 [m, 4H, $\text{N}(\text{CH}_2\text{CH}_2)_2$], 1.86-1.95 [m, 4H, $\text{N}(\text{CH}_2\text{CH}_2)_2$]. ^{13}C NMR (400.13 MHz, CDCl_3 , 298 K) δ 140.4 [C_{q}], 128.4 [CH], 128.2 [CH], 125.8 [CH], 58.2 [$\text{PhCH}_2\text{CH}_2\text{N}$], 54.0 [$\text{N}(\text{CH}_2\text{CH}_2)_2$], 35.8 [$\text{PhCH}_2\text{CH}_2\text{N}$], 23.4 [$\text{N}(\text{CH}_2\text{CH}_2)_2$].

Characterisation of 1-phenethylmorpholine (14): ^1H NMR (400.13 MHz, CDCl_3 , 298 K) δ 7.35-7.39 [m, 2H, H_{ar}], 7.28-7.3 [m, 3H, H_{ar}], 3.79 [t, 4H, $J = 4$ Hz, OCH_2], 2.88 [dd, 2H, $J = 4$ Hz, $J = 8$ Hz, $\text{PhCH}_2\text{CH}_2\text{N}$], 2.65 [dd, 2H, $J = 4$ Hz, $J = 8$ Hz, $\text{PhCH}_2\text{CH}_2\text{N}$], 2.54 [s, 4H, $\text{N}(\text{CH}_2\text{CH}_2)_2\text{O}$]. ^{13}C NMR (400.13 MHz, CDCl_3 , 298 K) δ 139.6 [C_{q}], 128.0 [CH], 127.7 [CH], 125.4 [CH], 66.2 [OCH_2], 60.2 [$\text{PhCH}_2\text{CH}_2\text{N}$], 53.1 [$\text{N}(\text{CH}_2\text{CH}_2)_2\text{O}$], 32.7 [$\text{PhCH}_2\text{CH}_2\text{N}$].

Synthesis of [(THF) $_2$ (NaMg(NC $_5$ H $_{10}$) $_3$)] $_2$ (15): [$\text{Na}(\text{CH}_2\text{SiCH}_3)$] (0.11 g, 1 mmol), [$\text{Mg}(\text{CH}_2\text{SiCH}_3)_2$] (0.22 g, 1 mmol) and hexane (10 mL) were added and stirred at room temperature during one hour. Piperidine (0.3 mL, 1 mmol) was added and the white suspension was stirred during one hour more at room temperature. THF (0.32 mL) was added and the suspension was gently heated until a clear solution was obtained and was placed to the freezer (-33 °C). After 24 hours the white solid was filtered and placed in a glovebox (0.185 g, 42%).

^1H NMR (400.13 MHz, C_6D_6 , 298 K) δ 2.06-1.77 [br. m, 12H, $\text{N}(\text{CH}_2\text{CH}_2)_2\text{CH}_2$], 1.74-1.46 [br m, 18H, $\text{N}(\text{CH}_2\text{CH}_2)_2\text{CH}_2 + \text{N}(\text{CH}_2\text{CH}_2)_2\text{CH}_2$].

^{13}C NMR ($\{^1\text{H}\}$) (100.62 MHz, C_6D_6 , 298 K) δ 55.1 [CH, $\text{N}(\text{CH}_2\text{CH}_2)_2\text{CH}_2$], 32.9 [CH, $\text{N}(\text{CH}_2\text{CH}_2)_2\text{CH}_2$], 28.2 [CH, $\text{N}(\text{CH}_2\text{CH}_2)_2\text{CH}_2$].

Elemental analysis: Due to the air and moisture sensitivity of the sample, elemental analysis experiments were unsuccessful.

Synthesis of [(THF) $_3$ (KMg(NC $_5$ H $_{10}$) $_3$)] $_2$ (16): To an oven dried Schlenk [$\text{K}(\text{CH}_2\text{SiCH}_3)$] (0.13 g, 1 mmol), [$\text{Mg}(\text{CH}_2\text{SiCH}_3)_2$] (0.22 g, 1 mmol) and hexane (10 mL) were added and stirred at room temperature during one hour. Piperidine (0.3 mL, 1 mmol) was added and the white suspension was stirred during one hour more at room temperature. THF (3 mL) was added and the suspension was gently heated until solution that was placed to the fridge overnight. Colourless crystals were obtained. The crystals were isolated and placed in a glovebox (0.245 g, 43%).

^1H NMR (400.13 MHz, C_6D_6 , 298 K) δ 3.47-3.19 [br. m, 12H, $\text{N}(\text{CH}_2\text{CH}_2)_2\text{CH}_2$], 1.42-1.55 [br. m, 6H, $\text{N}(\text{CH}_2\text{CH}_2)_2\text{CH}_2$], 1.15-1.39 [br. m, 12H, $\text{N}(\text{CH}_2\text{CH}_2)_2\text{CH}_2$].

^{13}C NMR ($\{^1\text{H}\}$) (100.62 MHz, C_6D_6 , 298 K) δ 55.5 [CH, $\text{N}(\text{CH}_2\text{CH}_2)_2\text{CH}_2$], 32.0 [CH, $\text{N}(\text{CH}_2\text{CH}_2)_2\text{CH}_2$], 28.4 [CH, $\text{N}(\text{CH}_2\text{CH}_2)_2\text{CH}_2$].

Elemental analysis: Due to the air and moisture sensitivity of the sample, elemental analysis experiments were unsuccessful.

Synthesis of [(TMEDA) $_2$ Na $_2$ Mg(NC $_5$ H $_{10}$) $_4$] (17): To an oven dried Schlenk [$\text{Na}(\text{CH}_2\text{SiCH}_3)$] (0.22 g, 2 mmol), [$\text{Mg}(\text{CH}_2\text{SiCH}_3)_2$] (0.20 g, 1 mmol) and hexane (10 mL) were added and stirred at room temperature during one hour. TMEDA (0.3 mL, 2 mmol) was added and the suspension was stirred during one hour. Piperidine (0.4 mL, 4 mmol) was added and the white suspension was stirred during one hour more at room temperature. The volume of the solution was halved by evaporation in vacuum and toluene (2 mL) was added. The suspension was gently heated until solution that was placed in a hot water bath. After 24 hours colourless crystals were obtained, isolated and placed in a glovebox (0.415 g, 65%).

^1H NMR (400.13 MHz, C_6D_6 , 298 K) δ 3.51 [m, 16H, $\text{N}(\text{CH}_2\text{CH}_2)_2\text{CH}_2$], 2.05 [m, 32H, $\text{N}(\text{CH}_2\text{CH}_2)_2\text{CH}_2 + (\text{CH}_3)$ TMEDA], 1.83 [s, 8H, (NCH $_2$) TMEDA], 1.69 [m, 16H, $\text{N}(\text{CH}_2\text{CH}_2)_2\text{CH}_2$].

^{13}C NMR ($\{^1\text{H}\}$) (100.62 MHz, d_8 -THF, 298 K) δ 57.3 [(CH $_2$) TMEDA], 55.6 [$\text{N}(\text{CH}_2\text{CH}_2)_2\text{CH}_2$], 46.2 [(CH $_3$) TMEDA], 32.8 [$\text{N}(\text{CH}_2\text{CH}_2)_2\text{CH}_2$], 28.7 [$\text{N}(\text{CH}_2\text{CH}_2)_2\text{CH}_2$].

Elemental analysis: ($\text{C}_{32}\text{H}_{72}\text{MgN}_8\text{Na}_2$) Calculated: C: 60.12 % H: 11.35 % N: 17.53 %. Found: C: 59.57 % H: 9.14 % N: 16.95 %.

Synthesis of [(PMDETA) $_2$ K $_2$ Mg(NC $_5$ H $_{10}$) $_4$] (18): To an oven dried Schlenk [$\text{K}(\text{CH}_2\text{SiCH}_3)$] (0.26 g, 2 mmol), [$\text{Mg}(\text{CH}_2\text{SiCH}_3)_2$] (0.20 g, 1 mmol) and hexane (10 mL) were added and stirred at room temperature during one hour. PMDETA (0.4 mL, 2 mmol) was added and the suspension was stirred during one hour. Piperidine (0.4 mL, 4 mmol) was added and a clear yellow solution was formed. After stirring for one hour at room temperature the solution was placed in the fridge. After 24 hours big yellow crystals were obtained, isolated and placed in a glovebox (0.3703 g, 47%).

^1H NMR (400.13 MHz, C_6D_6 , 298 K) δ 3.46 [m, 16H, $\text{N}(\text{CH}_2\text{CH}_2)_2\text{CH}_2$], 2.09 [s, 30H, (CH $_3$) PMDETA], 2.08 [m, 8H,

$N(CH_2CH_2)_2CH_2$], 2.02 [s, 16H, (NCH_2) PMDETA], 1.78 [m, 16H, $N(CH_2CH_2)_2CH_2$].

^{13}C NMR $\{^1H\}$ (100.62 MHz, d_8 -THF, 298 K) δ 57.5 [CH_2 PMDETA], 56.1 [$N(CH_2CH_2)_2CH_2$], 55.8 [CH_2 PMDETA], 45.8 [$(CH_3)_2$ PMDETA], 43.2 [(CH_3) PMDETA], 32.4 [$N(CH_2CH_2)_2CH_2$], 29.0 [$N(CH_2CH_2)_2CH_2$].

Elemental analysis: ($C_{38}H_{86}MgN_{10}K_2$) Calculated: C: 57.02 % H: 10.83 % N: 17.50 %. Found: C: 58.30 % H: 11.44 % N: 17.18 %.

Conclusions

Expanding wider the catalytic potential of s-block cooperative bimetallic reagents, this work establishes alkali-metal magnesiates as powerful catalyst to promote intermolecular hydroamination of diphenylacetylene and styrene. Reflecting the relevance on the nucleophilicity of the mixed-metal reagents, higher order (formally dianionic) magnesiates ($[(donor)_2AM_2Mg(CH_2SiMe_3)_4]$ AM = Li, Na, K) proved to be efficient catalysts, capable of promoting hydroamination processes at room temperature, while lower-order ($[AMMg(CH_2SiMe_3)_3]$ AM = Li, Na, K) require harsher reaction conditions (80 °C and long timescales). Interestingly, a pronounced alkali-metal effect is observed in higher order magnesiate precatalysts, with the K/Mg partnership being the most efficient of them all, mediating the smooth hydroamination of styrene at room temperature in 15 minutes. These findings contrast with the complete lack of activity shown by $[Mg(CH_2SiMe_3)_2]$. Initial reactivity and structural studies suggest that the role of the alkali metal is to act as a potent Lewis acid, coordinating the unsaturated organic molecule to facilitate the addition of an amide anion. X-ray crystallography combined with 1H DOSY NMR experiments have been used to help identify important reaction intermediates. These initial stoichiometric studies suggest similar mechanisms to those proposed for calcium or strontium catalysis.

Conflicts of interest

The authors confirm there are no conflicts of interest to declare.

Acknowledgements

We thank the European Research Council (ERC-Stg Mixmetapps to EH) for its generous sponsorship. Authors also thank R. E. Mulvey for his insightful comments.

Notes and references

† Electronic Supplementary Information (ESI) available: Providing experimental procedures, NMR spectra and crystallographic data.

- (a) J. Seayad, A. Tillack, C. G. Hartung and M. Beller, *Adv. Synth. Catal.*, 2002, **344**, 795–813; (b) A. L. Reznichenko, K. C. Hultzs, in *Top Organomet Chem* (Eds.: V. P. Ananikov and M. Tanaka), Springer Berlin Heidelberg, 2013, pp. 51–114; (c) T. E. Müller, K. C. Hultzs, M. Yus, F. Foubelo and M. Tada, *Chem. Rev.*, 2008, **108**, 3795–3892; (d) J. Hannedouche and E. Schulz, *Chem. Eur. J.*, 2013, **19**, 4972–4985; (e) T. E. Müller and M. Beller, *Chem. Rev.*, 1998, **98**, 675–703; (f) R. Severin and S. Doye, *Chem. Soc. Rev.*, 2007, **36**, 1407–1420.
- (a) M. Beller, C. Breindl, T. H. Riermeier, M. Eichberger and H. Trauthwein, *Angew. Chem. Int. Ed.*, 1998, **37**, 3389–3391; (b) S. M. Coman and V. I. Parvulescu, *Org. Process Res. Dev.*, 2015, **19**, 1327–1355; (c) R. Hili and A. K. Yudin, *Nat. Chem. Biol.*, 2006, **2**, 284–287; (d) S.-L. Shi and S. L. Buchwald, *Nat. Chem.*, 2015, **7**, 38–44.
- (a) J. Penafiel, L. Maron and S. Harder, *Angew. Chem. Int. Ed.*, 2015, **54**, 201–206; (b) M. Beller, J. Seayad, A. Tillack and H. Jiao, *Angew. Chem. Int. Ed.*, 2004, **43**, 3368–3398.
- (a) L. Huang, M. Arndt, K. Gooßen, H. Heydt and L. J. Gooßen, *Chem. Rev.*, 2015, **115**, 2596–2697; (b) F. Alonso, I. P. Beletskaya and M. Yus, *Chem. Rev.*, 2004, **104**, 3079–3159.
- (a) S. Harder, *Chem. Rev.*, 2010, **110**, 3852–3876; (b) A. G. M. Barrett, C. Brinkmann, M. R. Crimmin, M. S. Hill, P. Hunt and P. A. Procopiou, *J. Am. Chem. Soc.*, 2009, **131**, 12906–12907; (c) M. R. Crimmin, I. J. Casely and M. S. Hill, *J. Am. Chem. Soc.*, 2005, **127**, 2042–2043; (d) M. S. Hill, D. J. Liptrot and C. Weetman, *Chem. Soc. Rev.*, 2016, **45**, 972–988; (e) C. Brinkmann, A. G. M. Barrett, M. S. Hill and P. A. Procopiou, *J. Am. Chem. Soc.*, 2012, **134**, 2193–2207.
- B. Liu, T. Roisnel, J.-F. Carpentier and Y. Sarazin, *Angew. Chem. Int. Ed.*, 2012, **51**, 4943–4946.
- (a) S. Hong and T. J. Marks, *Acc. Chem. Res.*, 2004, **37**, 673–686; (b) J.-S. Ryu, G. Y. Li and T. J. Marks, *J. Am. Chem. Soc.*, 2003, **125**, 12584–12605.
- (a) P. Horrillo-Martínez, K. C. Hultzs, A. Gil and V. Branchadell, *Eur. J. Org. Chem.*, 2007, 3311–3325; (b) R. Wegler and G. Pieper, *Chem. Ber.*, 1950, **83**, 1–6; (c) R. J. Schlott, J. C. Falk and K. W. Narducy, *J. Org. Chem.*, 1972, **37**, 4243–4245; (d) D. Tzalis, C. Koradin and P. Knochel, *Tetrahedron Lett.*, 1999, **40**, 6193–6195; (e) G. P. Pez and J. E. Galle, *Pure Appl. Chem.*, 1985, **57**, 1917–1926; (f) B. W. Howk, E. L. Little, S. L. Scott and G. M. Whitman, *J. Am. Chem. Soc.*, 1954, **76**, 1899–1902.
- See for example: (a) N. P. Mankad, *Chem. Eur. J.*, 2016, **22**, 5822–5829; (b) J. Park and S. Hong, *Chem. Soc. Rev.*, 2012, **41**, 6931–6943.
- For some recent examples using mixed Li/Al systems to promote hydroboration reactions see: (a) V. A. Pollard, S. A. Orr, R. McLellan, A. R. Kennedy, E. Hevia and R. E. Mulvey, *Chem. Commun.*, 2018, **54**, 1233–1236; (b) L. E. Lemmerz, R. McLellan, N. R. Judge, A. R. Kennedy, S. A. Orr, M. Uzelac, E. Hevia, S. D. Robertson, J. Okuda and R. E. Mulvey, *Chem. Eur. J.*, 2018, **24**, 9940–9948; (c) V. A. Pollard, M. Ángeles Fuentes, A. R. Kennedy, R. McLellan and R. E. Mulvey, *Angew. Chem. Int. Ed.*, 2018, **57**, 10651–10655.
- A. Hernán-Gómez, T. D. Bradley, A. R. Kennedy, Z. Livingstone, S. D. Robertson and E. Hevia, *Chem. Commun.*, 2013, **49**, 8659–8661.
- M. De Tullio, A. Hernán-Gómez, Z. Livingstone, W. Clegg, A. R. Kennedy, R. W. Harrington, A. Antiñolo, A. Martínez, F. Carrillo-Hermosilla and E. Hevia, *Chem. Eur. J.*, 2016, **22**, 17646–17656.
- (a) C. Glock, H. Görls and M. Westerhausen, *Chem. Commun.*, 2012, **48**, 7094–7096; (b) C. Glock, F. M. Younis, S. Ziemann, H. Görls, W. Imhof, S. Kriek and M. Westerhausen, *Organometallics*, 2013, **32**, 2649–2660; (c) F. M. Younis, S. Kriek, H. Görls and M. Westerhausen, *Organometallics*, 2015, **34**, 3577–3585; (d) F. M. Younis, S. Kriek, H. Görls and M. Westerhausen, *Dalton Trans.*, 2016, **45**, 6241–6250.
- (a) S. E. Baillie, W. Clegg, P. García-Álvarez, E. Hevia, J. Klett and L. Russo, *Organometallics*, 2012, **31**, 5131–5142; (b) S. E. Baillie, W. Clegg, P. García-Álvarez, E. Hevia, A. R. Kennedy, J. Klett and L. Russo, *Chem. Commun.*, 2011, **47**, 388–390.

- 15 (a) V. Butera, N. Russo and E. Sicilia, *Chem. Eur. J.*, 2014, **20**, 5967–5976 (b) M. S. Hill, M. Hodgson, D. J. Liptrot and M. F. Mahon, *Dalton Trans.*, 2011, **40**, 7783–7790; (c) D. J. Liptrot, M. S. Hill, M. F. Mahon and D. J. MacDougall, *Chem. Eur. J.*, 2010, **16**, 8508–8515.
- 16 (a) N. D. R. Barnett, R. E. Mulvey, W. Clegg and P. A. O’Neil, *J. Am. Chem. Soc.*, 1991, **113**, 8187–8188; (b) W. Clegg, B. Conway, A. R. Kennedy, J. Klett, R. E. Mulvey and L. Russo, *Eur. J. Inorg. Chem.*, 2011, 721–726.
- 17 R. E. Mulvey, F. Mongin, M. Uchiyama and Y. Kondo, *Angew. Chem. Int. Ed.*, 2007, **46**, 3802–3824.
- 18 S. E. Baillie, T. D. Bluemke, W. Clegg, A. R. Kennedy, J. Klett, L. Russo, M. de Tullio and E. Hevia, *Chem. Commun.*, 2014, **50**, 12859–12862.
- 19 (a) K. D. Hesp and M. Stradiotto, *J. Am. Chem. Soc.*, 2010, **132**, 18026–18029; (b) A. Reyes-Sánchez, I. García-Ventura and J. J. García, *Dalton Trans.*, 2014, **43**, 1762–1768.
- 20 V. M. Arredondo, S. Tian, F. E. McDonald and T. J. Marks, *J. Am. Chem. Soc.*, 1999, **121**, 3633–3639.
- 21 (a) D. R. Armstrong, H. S. Emerson, A. Hernán-Gómez, A. R. Kennedy and E. Hevia, *Dalton Trans.*, 2014, **43**, 14229–14238; (b) R. E. Mulvey, *Chem. Commun.*, 2001, 1049–1056.
- 22 (a) E. Weiss and D. Kristallstruktur, *Chem. Ber.*, 1968, 35–40; (b) E. Weiss and G. Hencken, *J. Organomet. Chem.*, 1970, **21**, 265–268.
- 23 R. Neufeld and D. Stalke, *Chem. Sci.*, 2015, **6**, 3354–3364.
- 24 R. A. Lewis, G. Wu and T. W. Hayton, *Inorg. Chem.*, 2011, **50**, 4660–4668.
- 25 (a) W. Clegg, K. W. Henderson, R. E. Mulvey and P. A. O’Neil, *Chem. Commun.*, 1993, 969–970; (b) W. Clegg, K. W. Henderson, R. E. Mulvey and P. A. O’Neil, *J. Chem. Soc., Chem. Commun.*, 1994, 769–770.
- 26 G. M. Sheldrick, *Acta Crystallogr.*, 2007, **A64**, 112–122.